New Operator Based on a Multi Support Point Algorithm Applied to Feature Extraction

Michel Bilodeau, Estelle Parra-Denis, Dominique Jeulin

NEW OPERATOR BASED ON A MULTI SUPPORT POINT ALGORITHM APPLIED TO FEATURE EXTRACTION

Michel Bilodeau, *Estelle Parra-Denis* and *Dominique Jeulin*

Mines Paristech, CMM-Centre de Morphologie Mathématique, Mathématique et Systèmes, Fontainebleau, France
(Draft from November 5, 2013)

ABSTRACT

In the context of quality control, we propose a new operator using multi support points to highlight local perturbations on flat surfaces. We compare the design of this operator with different gradients and residues in their ability to extract small perturbations as well as their efficiency on large surface.
The operator is defined as a weighted differential operator evaluated on each point. It is designed to extract a region with a high slope followed by a plateau with a given width. It has a low computational complexity and it could be vectorized

KEYWORDS: Feature extraction, laplacian of gaussian, tophat transform, mathematical morphology, blob detection.

Introduction

Feature extraction are common image processing techniques used in manufacturing for quality and process control. In quality control, it is usually performed with an *a priori* knowledge of the inspect material, so the task of finding defects could be transcribed in terms of finding, with the proper feature extractors, discontinuities in depth, size, surface or material properties. In textile, metal sheet or raw material manufacturing, the surface inspection is often complex and requires a large number of detectors as defects don't have a single signature. With the number of detectors increasing, there is a demand to more efficient and effective algorithms, even at the lowest level.

In this paper, we propose a simple algorithm to highlight local perturbation on a flat surface. It belongs to the blob detector category, with the Lindeberg definition of *blob* where a bright/dark blob is the region associated to a local maximum/minimum.

Currently, there are two trends in detection of grey blobs. One is to find the edges of the blob. The other trend is based on the extrema. The laplacian of gaussian (LoG) is representative of the first trend, while the opening of residues, also called top-hat transform, is representative of the second one.

Blob detectors

To illustrate the performance of the blob detectors and ease their comparison, we will show their result on a 1-D profile. This profile is made from three gaussians of σ equals to $21, 50, 100$.

Laplacian of gaussian

The laplacian operator is used to detect edges, but it is seldom used that way directly since it is too sensible to noise. It was found by Marr and Poggio in [8] that a convolution by a gaussian followed by the laplacian was giving better result and it has also good properties: it scales well, it is localized spatially and it has limited band-width. Direction of intensity changes can also be given by the laplacian. Giving a gaussian G with a width of σ :

$$G_\sigma(x,y) = \frac{1}{2\pi\sigma^2} e^{\frac{x^2+y^2}{2\sigma^2}}, \tag{1}$$

the laplacian of gaussian (LoG) of an image I is simply:

$$LoG((x,y) = \sigma^2 \nabla^2 G_\sigma \star I(x,y) \tag{2}$$

The LoG can also be approximated and implemented as a difference of two gaussians of difference size:

$$DoG(x,y) = G_\sigma \star I(x,y) - G_{k\sigma} I(x,y), \tag{3}$$

where k is a ratio factor between the two gaussians. With $k \simeq 1.6$, the equations 2 and 3 give similar results [8]

The LoG scales well, as we need only to change σ to extract blob of different sizes, but practically, to extract a large range of sizes of blobs, other schemes are used, like a multi-scale approach. One famous is part of Sift algorithm from Lowe [7], where the LoG are computed by DoG two-by-two at different scale-space and then analysed to find the most revelant one.

The figure 1 shows a result of LoG performed on the 1-D profile. Interesting points of interests of the LoG are its maxima which would indicate a blob at these position and the zero-crossings which indicate edges of a blob. We can see on this figure that the blob at the left with narrow peak could be extracted with a $\sigma = 30$, while the peak at the right could not.

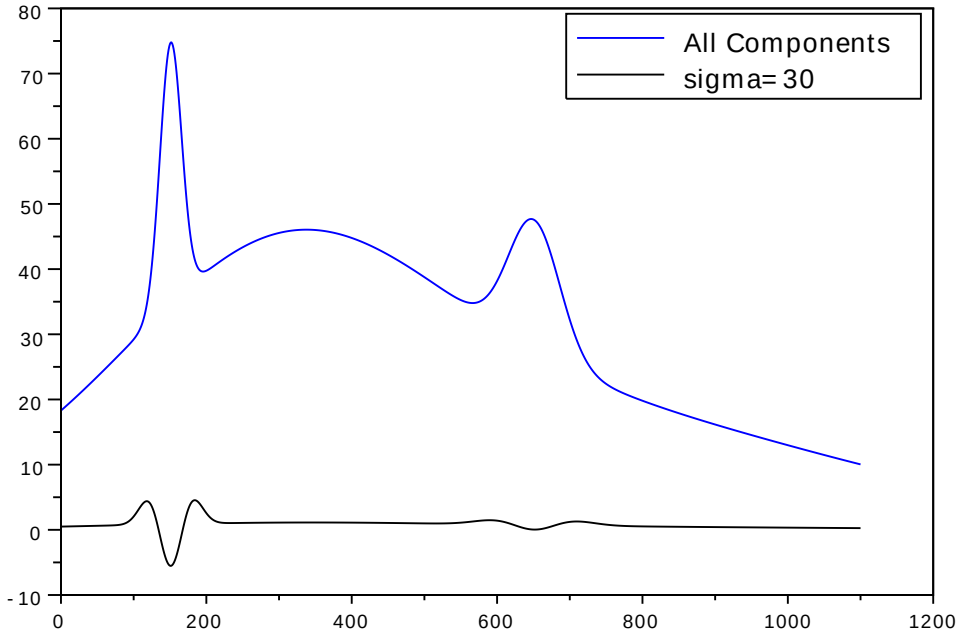

Fig. 1: *Laplacian of gaussian (LoG). In blue, the original profile, in black the LoG* $\sigma = 30$

Top-hat transform

The top-hat transform is as well known operator in mathematical morphology [10] and was used by Meyer [9] in a cytology application. It is not a symetrical function as the LoG, as it detects only one phase at a time: dark regions or clear one, not both. The top-hat is built with opening to detect white blobs or with closing to detect dark blobs as follow:

$$TopW_s(x,y) = I(x,y) - \gamma_s(x,y), \tag{4}$$

for the white tophat, and

$$TopB_s(x,y) = \phi_s(x,y) - I(x,y), \tag{5}$$

for the black tophat. The symbols γ is the opening function, ϕ the closing function. The parameter s is the size of the structuring element which is the shape of the neighborhood that is being probe.

The opening is used to filter out white peaks of an image. Once subtract from the image, the white peaks remain. Figure 2 illustrates the white tophat with two different sizes of structuring element. The behaviour of the tophat is simple: at each point of the profile, you are looking if all the neighbors described by the structured element have a value inferior or equal. If it is, that point is part of the tophat.

In the figure 2, two peaks are partly detected. This is the part of peak with width lower to 25 pixels. A the bottom of this figure, all peaks are detected. The tophat is similar to the *LoG* as it scales well by changing the size of the structuring element. But contrary to the *LoG* it is not a narrow-band filter, but an high-pass filter. For an increasing size of filter, you are getting more and more blobs. Similar to the *LoG*, multi-space approach has also been used in [2, 4, 3]. One of the big advantage of the tophat over the *LoG* is that it possible to select blobs, not only by their size, but also by their depth as the relative heights of the peaks are preserved.

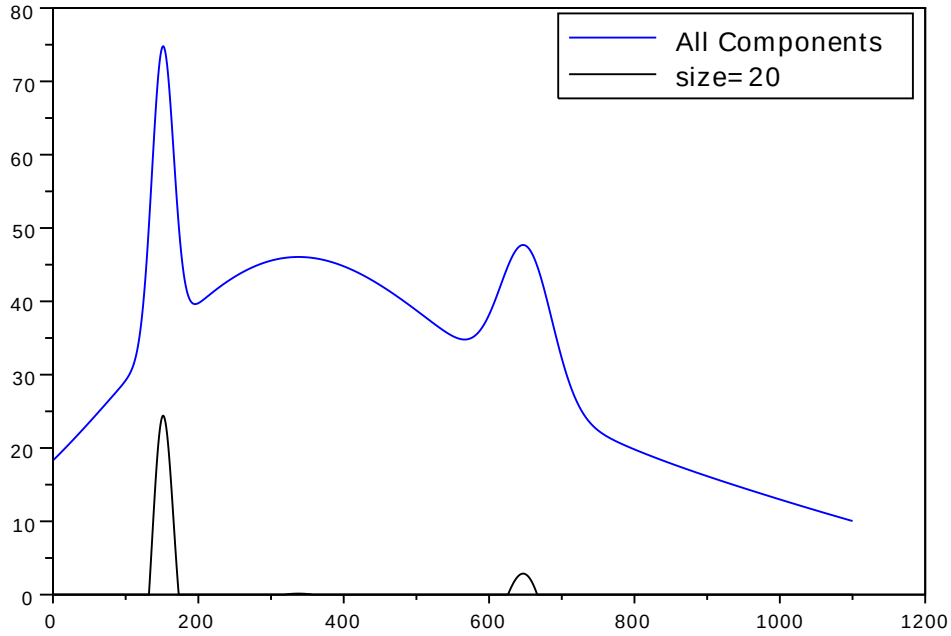

Fig. 2: *Results of tophat with size=25. Result in black. Original in blue.*

Multi-points detector

Both the tophat and the *LoG* are time consuming for the detection of large blobs. Although very good algorithms have been developed to incresease the speed of these detectors [11, 1], they are still dependent of the number of pixels in the neighborhood.

The proposed detector[5], that we call here multi-points detector, relies only on few points. It was designed to detect blobs of a certain size on a material where it should not have any.

For simplicity, the explanation that follows is in 1-D. It can be extend in 2-D as well. At each point x of the image $g(x)$, we are looking at 4 points at a distance of a and b from x. Let $(x-a)$, $(x+a)$, $(x-b)$ and $(x+b)$ be those points, with $a > b > 0$. Let make the hypothesis that x is at a center of blob. The area at the top of the blob should correspond to a region with a low gradient. This inner gradient is evaluated between the center and its two close probing points with $|g(x)-g(x-b)|$ and $|g(x)-g(x+b)|$. The points at the edge of the blob should be at a strong gradient. This outer gradient can be evaluated between the external probing points as $|g(x-a)-g(x-b)|$ and $|g(x+a)-g(x+b)|$. Now to verify the hypothesis, we need to maximize

the expression:

$$\begin{aligned} f(x,a,b) = |g(x-a) - g(x-b)| + \\ |g(x+a) - g(x+b)| - \\ |g(x) - g(x-b)| - \\ |g(x) - g(x+b)| \end{aligned} \tag{6}$$

Equation 6 could be re-written as four convolutions with a sparse kernel matrice:

$$\begin{aligned} f(x,a,b) = |g \star K_{a,b}| + |\star K_{a,-b}| - \\ |g \star K_{-b}| - |g \star K_{+b}|, \end{aligned} \tag{7}$$

where K_{xx} are sparce kernels containing the weights:

$$\begin{aligned} K_{-a,-b} = (1 \ldots\ldots -1 \ldots\ldots 0 \ldots\ldots\ldots\ldots\ldots) \\ K_{-b} = (0 \ldots\ldots -1 \ldots\ldots 1 \ldots\ldots\ldots\ldots\ldots) \end{aligned} \tag{8}$$

the others are just transposed. That formulation is very convenient: we can easily imagine to change the weights 1 by something else. The physical sense is that you put more weights to one group of gradients of eq.6 relative to the other ones: favor a less strong gradient at the top of the blob, or not.

We can see on figures 3 through 4 results of the detector applied to the test profile. On figure 3, we can see a good response of the detector for the narrow peak at the left. The parameter $a = 40$ was selected to be a bit larger than the width of that blob. In figure 4, with $a = 100$, the blob at the right starts to have a good response, while the response at the left is getting wider: it is because we are getting the response of the middle dome. We can see at the top of that figure, the individual response of the three blobs as if they were alone. We can reduce the influence of the dome by increasing the parameter b. The figure 5 gives the result.

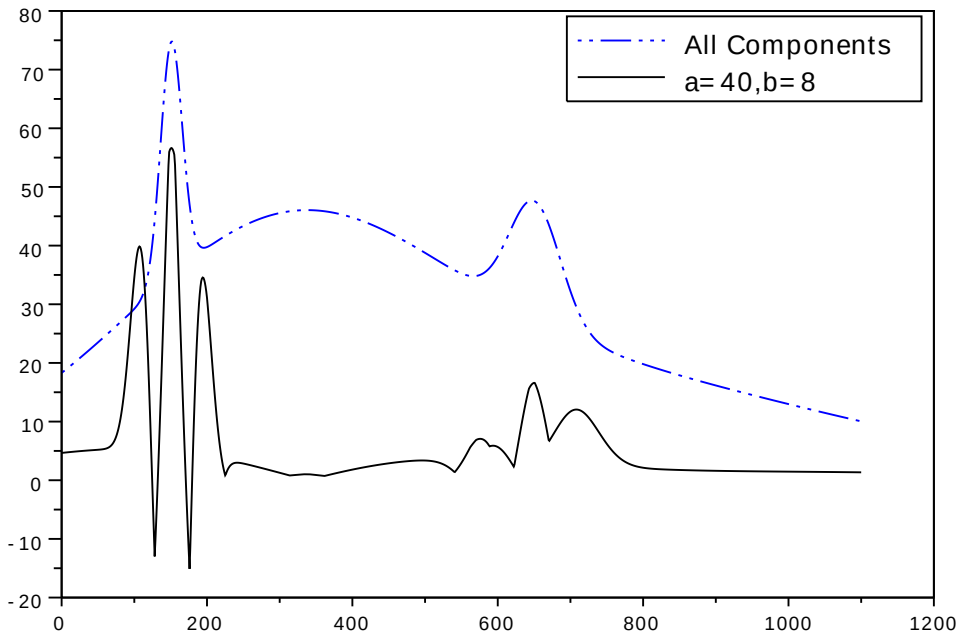

Fig. 3: *Multi-points detector with $a = 40, b = 8$. The original in blue dot-line, and the detector response in black.*

We studied the influence of random noise and high fluctuation on the blob detection. It seems reasonably stable.

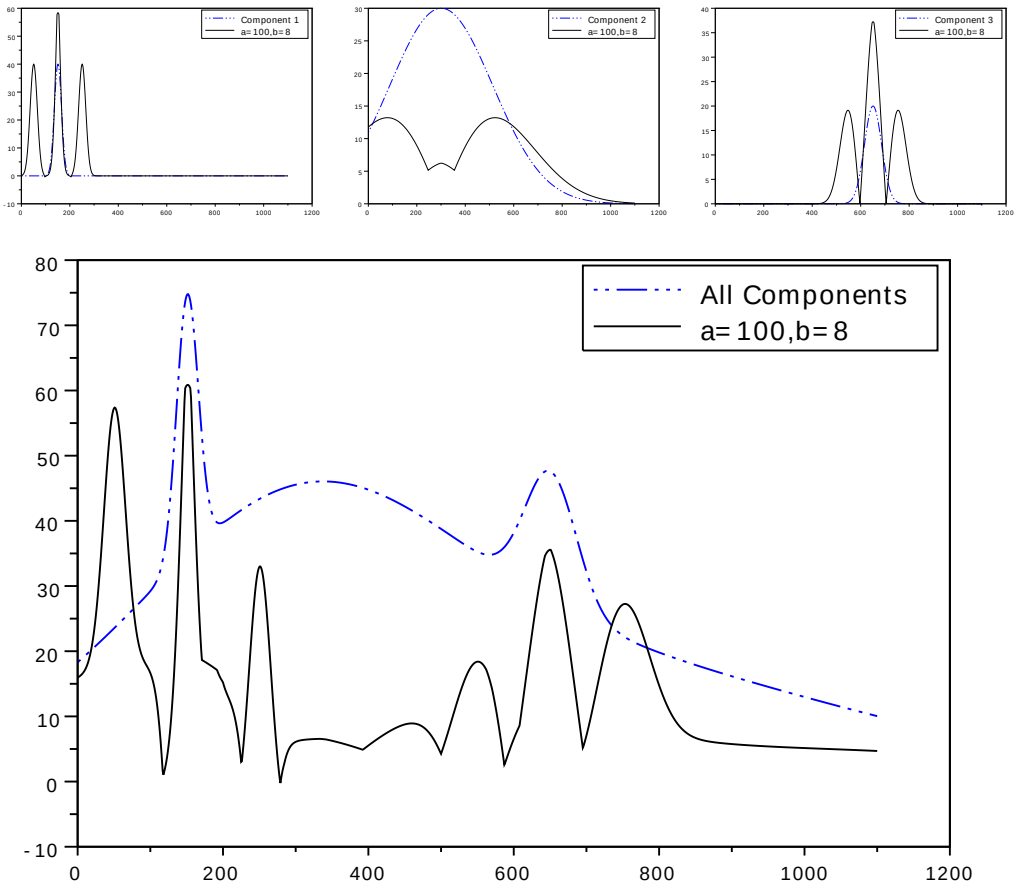

Fig. 4: *Multi-points detector with* $a = 100, b = 8$. *At the bottom the original is in blue dot-line, and the detector response in black. At the top, three imagets containing the three individuals components of the profile with their respective detector response*

Test case

We try all the dectors on images of a textile taken with a 3d-camera similar to Sick 3d camera system [12]. That kind of camera gives a matrice of altitude instead of luminance. We can see the image test case in 6a as a 3d surface plot. The textile is flexible, explaining big differences in altitude. The blob to detect is the the red circle. It is not so well expressed compared to the dynamic of the whole image, but it is noticable. The figure 6b gives the ouput of the *LoG* operator. The blob is enhanced, but is still difficult to extract it, as the textile bending has been increase. The figure 6c gives the ouput of the tophat. The blob is very well detected. Notice, that dynamic has been shrunk to the relative height of the bob. Finally, we can the result of the multi-point detector on figure 6c. The detector gives a very good response with the selected parameter.

For this kind of images with few blobs on a bending surface, we obtain comparable results to a tophat transform. Like the tophat, we need to fit the parameters to match the blob size and depth. It is however faster than the tophat as it needs only to read 5 points for each produced pixels while the tophat has to manage a neighborhood proportional to the size of the blob and make a computation over that neighborhood. In this test case that neighborhood size is 100.

Conclusion

The proposed multi-points detectors shows promising results on the images we studied. It is a good symmetrical scalable blob detector, comparable in the studied image to the tophat, although

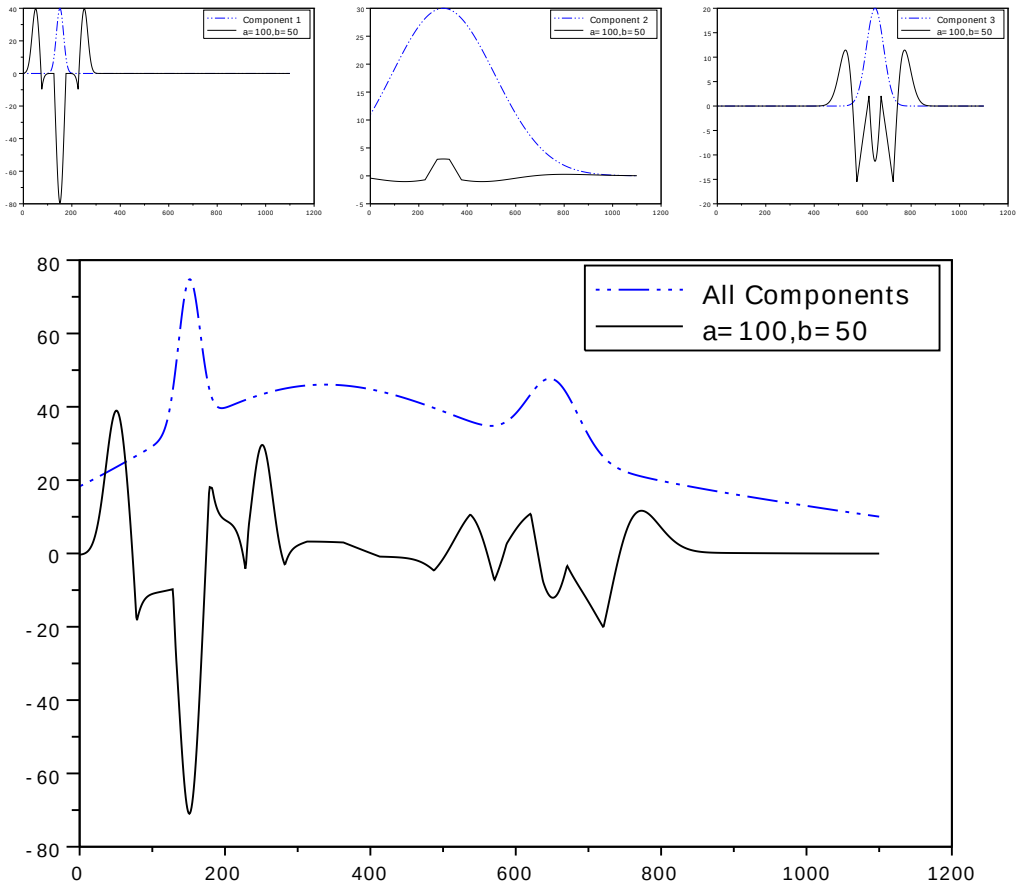

Fig. 5: *Multi-points detector with* $a = 100, b = 50$*. At the bottom the original is in blue dot-line, and the detector response in black. At the top, three imagets containing the three individuals components of the profile with their respective detector response*

we still need to do more test cases. The next step in the development of this algorithm is to adapt a multi-scale approach.

References

[1] Crowley, J. , Riff, O. (2003). Fast computation of scale normalised Gaussian receptive fields. In Scale Space (pp. 584–598).

[2] J. A. Bangham, P. D. Ling, R. Harvey, Scale-space from nonlinear fiters, IEEE Trans. Pattern Anal. Machine Intell. 18 (1996) 520–528.

[3] Florence, L., Guy, F., Olivier, A. (2011). The Morphological Pyramid and it Applications to Remote Sengin: Multiresolution Data Analysis and Features Extraction. Image Analysis & Stereology, 21(1), 49-53. doi:10.5566/ias.v21.p49-53

[4] J. Goutsias, H. J. A. M. Heijmans, Multiresolution signal decomposition schemes. Part 1: Linear and morphological pyramids, IEEE Trans. Image Processing 9 (11) (2000) pp 1862-1876.

[5] Jeulin D. (2010) Extraction de bosses sur des profils, N-09/10/MM, Internal report, Paris School of Mines.

[6] Lindeberg, T. (1991) Discrete Scale-Space Theory and the Scale-Space Primal Sketch, PhD thesis, Department of Numerical Analysis and Computing Science, Royal Institute of Technology, S-100 44 Stockholm, Sweden, May 1991.

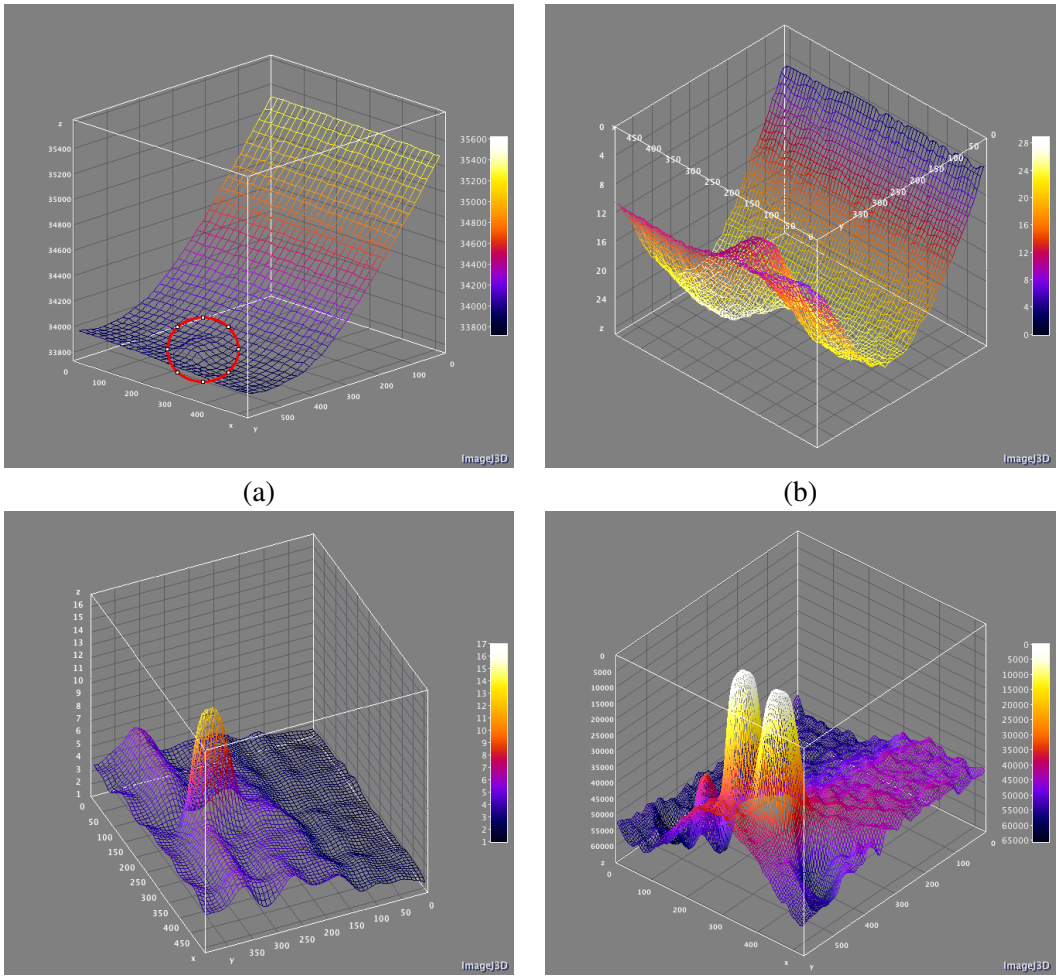

Fig. 6: *Surface plot of the results. (a) original image. the blob to detect is in the red circle (b) LoG with* $\sigma = 80$*, (c) top-hat transform with size* $= 100$ *, (d) multi-points detector with* $a = 200, b = 100$

[7] Lowe, D. G. (2004). Distinctive image features from scale-invariant keypoints. Inter- national Journal of Computer Vision, 60(2), pp 91-110.

[8] Marr David, Poggio T. 1979 A computational theory of human stereo vision. Proc. R. Soc. Lond. B 204, 301-328.

[9] Meyer F. , Cytologie quantitative et morphologie mathématique. Thèse docteur-ingénieur. Ecole des Mines de Paris, Paris, 1979

[10] Serra J., Image Analysis and Mathematical Morphology Vol. I , Ac. Press, London, 1982, 600 pages.

[11] van Herk, M. Pattern Recogn. Lett., Elsevier Science Inc., 1992, 13, pp 517-52

[12] Trademark of Sick AG See http://www.sick.com/ivp